Research Article

Optimal Design and Dynamic Performance Analysis of Vehicle Suspension Employing an Eccentric Inerter

Chengqun Qiu [1,2] **Ang Chen,**[2] **Yuqiu Xu,**[2] **and Yujie Shen** [2]

[1]*Jiangsu Province Intelligent Optoelectronic Devices and Measurement-Control Engineering Research Center,*
Yancheng Teachers University, Yancheng 224007, China
[2]*Automotive Engineering Research Institute, Jiangsu University, Zhenjiang 212013, China*

Correspondence should be addressed to Yujie Shen; shenyujie@ujs.edu.cn

This paper concerns the dynamic performance analysis of the vehicle ISD (inerter-spring-damper) suspension employing an eccentric inerter. Firstly, the quarter car model of the two basic vehicle suspension layouts involving an eccentric inerter, namely, the series-connected layout and the parallel-connected layout, is established. Then, by considering the overall performance such as the vehicle body acceleration, the suspension working space, and the dynamic tire load, the key parameters of the two suspensions are optimized by using the genetic algorithm. Simulation analysis results indicate that the series-connected vehicle ISD suspension is superior to the parallel-connected one, and all of the RMS values of the body acceleration, the suspension working space, and the dynamic tire load are decreased significantly by comparing to the conventional suspension, while the improvement of the parallel-connected vehicle ISD suspension is relatively poor. At last, the impact of the flywheel eccentricity and the screw pitch on the dynamic performance indices of the two suspensions is discussed, and the trade-offs among the three performances are analyzed, which will provide a guide method for the suspension design when considering the eccentric factor.

1. Introduction

Vehicle suspension is the general term for power transmission devices between wheels and the vehicle body. Suspension performance has an important impact on the vehicle's ride comfort, handling stability, and driving safety. Until now, semiactive suspension [1–3] and active suspension [4–6] systems have been widely known and used in high-class passenger cars, which make up for the shortcomings of the traditional passive suspension that cannot dynamically and adaptively adjust according to the external input or the change of the vehicle state. Recently, a new kind of passive vehicle suspension system employing the inerter, a new mechanical element, has been heatedly discussed.

Professor Smith from Cambridge University proposed the concept of "inerter" in 2002 [7], which is a two-terminal mechanical element with the defining property that the relative acceleration between the two terminals is proportional to the force applied to the terminals. It was shown that

the inerter element has a simple structure and excellent vibration absorption performance. In the area of vehicle suspension, the inerter-spring-damper (ISD) suspension system showed excellent comprehensive vibration reduction performance compared with the traditional passive suspension, especially the semiactive suspension with semiactive inerter [8–10]. Compared with controllable suspensions such as active suspension and semiactive suspension, the ISD suspension system using the inerter does not require energy input and does not depend on the control system, which can effectively reduce energy consumption, greatly reduce the complexity of the system, enhance the effectiveness and real-time performance of the system, improve the reliability of the system, fundamentally solve the gap between the actual performance and the theoretical performance of the active and semiactive systems, and improve the comprehensive performance of the vehicle [11].

Besides the vehicle suspension, the inerter element has been successfully deployed in other areas as well, for

example, in the area of civil engineering, three different types of inerter-based dampers (IBD), namely the tuned viscous mass damper (TVMD), the tuned mass damper inerter (TMDI), and the tuned inerter damper (TID), were studied, and these IBDs were found effective in seismic response control of structures [12–15]. In the area of railway suspension, an inerter is widely used in the design of train suspension systems. Research shows that the performance of train suspension systems can be improved by combining inerters with the traditional suspension elements [16–18].

Generally, there are many realizations of inerters, such as the ball-screw inerter [19], the rack-and-pinion inerter [20], the hydraulic inerter [21], and the fluid inerter [22]. In [23], in order to design a comfortable-oriented vehicle suspension structure, the network synthesis method was utilized to transfer the problem into solving a timing robust control problem and determine the structure of an "inerter-spring-damper" suspension. In [24], a new hydraulically interconnected inerter-spring-damper suspension (HIISDS) has been developed to compensate for traditional passive suspension limitations, such as the imbalance of ride performance and handling stability, and the effectiveness of HIISDS has been verified by simulation results. Yang [25] combines the concepts of using an acceleration-driven-damping (ADD) approach and an ISD passive network to isolate a wider frequency of vibrations in a vehicle suspension system, and the results demonstrate that the controllable ISD suspension system based on the ADD positive real network can enhance the vibration suppression of medium-high frequency bands based on the ISD suspension and thus comprehensively improve suspension performance.

However, most studies in the field of ISD suspension have only focused on the optimization of the suspension structure and improvement of the control strategy [26–29], and few researchers have treated to improve the structure of the inerter itself in much detail. It can be seen from the existing research that the structure of the inerter is diverse, and most structures tend to be idealized, ignoring the presence of eccentric devices in many scenarios. Besides, through the application of an eccentric inerter, the effect is different from the traditional model under the same road input, and some more favorable conclusions can be obtained. Therefore, the inerter with an eccentric structure needs to be studied emphatically. Considering that most inerters use flywheels to encapsulate inertia, this paper will propose an inerter with an eccentric flywheel structure and then explore the performance of ISD suspension with an eccentric inerter. The paper is arranged as follows:

In Section 2, a new inerter structure with an eccentric flywheel is proposed, and the vehicle ISD suspension model with series-connected and parallel-connected eccentric inerters is built. In Section 3, optimizations are finished in the condition of random road input using the genetic algorithm. In Section 4, simulation analysis of the two suspension models will be carried out both in the time domain and the frequency domain, and the impact of the variations of the flywheel eccentricity and the screw pitch on the suspension performance is discussed in detail in Section 5. Finally, some conclusions are drawn in Section 6.

2. Establishment of Vehicle Suspension

2.1. Introduction of the Eccentric Inerter. Traditional inerters used in vehicle suspension systems are mostly noneccentric flywheel structures, and this paper will focus on a ball-screw inerter employing an eccentric flywheel, which works as follows: when the suspension system generates up and down vibration, the upper and lower lugs produce relative linear motion, the ball screw and the screw nut convert the linear motion into the rotary motion of the screw, and the screw drives the eccentric flywheel to rotate and encapsulate the flywheel inertia. Figure 1 shows the schematic of the eccentric inerter studied in this paper.

In Figure 1(a), 1 is the up-lug, 2 is the screw, 3 is the screw nut, 4 is the down-stroke-room, 5 is the up-stroke-room, 6 is the support structure, 7 is the eccentric flywheel, and 8 is the down-lug. The 3D model schematic of the eccentric inerter is shown in Figure 1(b). The mass of the eccentric flywheel is m, the radius is r, the eccentricity of the flywheel is e, and the pitch of the ball screw is p, then the rotational inertia of the eccentric flywheel can be expressed as

$$I = \frac{1}{2}mr^2 + me^2. \tag{1}$$

According to the relevant principles of the ball-screw inerter, the inertance of this inerter is

$$b = \left(\frac{1}{2}mr^2 + me^2\right) \times \left(\frac{2\pi}{p}\right)^2. \tag{2}$$

2.2. Establishment of the ISD Suspension with an Eccentric Inerter (Two Layouts). In this section, a typical quarter car suspension model is considered, which can effectively show the relative motion between the sprung mass and the unsprung mass, with the spring and damper in parallel connection. Two basic vehicle suspension layouts, called series-connected suspension and parallel-connected suspension employing the eccentric inerter element, are introduced as shown in Figures 2 and 3.

In Figure 2, m_s is the sprung mass, m_u is the unsprung mass, k is the stiffness of the spring, c is the damping coefficient, k_t is the stiffness of the tire spring, and z_s, z_u, and z_r are the vertical displacements of the sprung mass, unsprung mass, and road input, respectively.

For the sprung mass m_s, according to Newton's laws of kinematics, the equation is

$$m_s\ddot{z}_s + k(z_s - z_u) + \left[\left(\frac{1}{2}mr^2 + me^2\right) \times \left(\frac{2\pi}{p}\right)^2\right](\ddot{z}_s - \ddot{z}_b) = 0. \tag{3}$$

For the unsprung mass m_u, the equation is

$$m_u\ddot{z}_u + k(z_u - z_s) + c(\dot{z}_u - \dot{z}_b) + k_t(z_u - z_r) = 0. \tag{4}$$

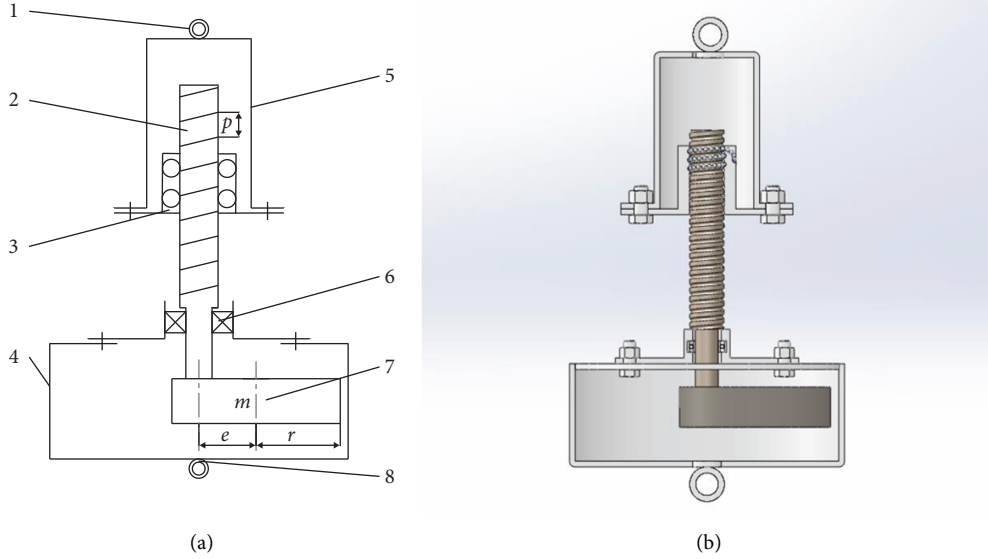(a)   (b)

FIGURE 1: Schematic of the eccentric inerter.

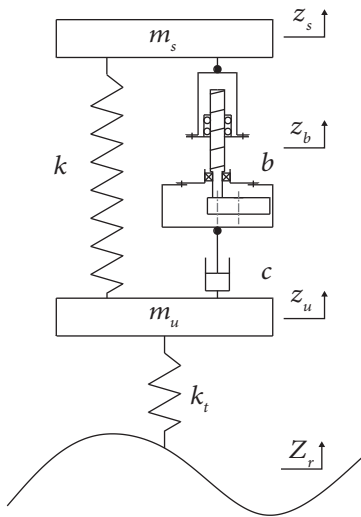FIGURE 2: The vehicle ISD suspension model with series-connected eccentric inerters.

FIGURE 3: The vehicle ISD suspension model with parallel-connected eccentric inerters.

For the point where the eccentric inerter is connected to the damping, the equation is

$$\left[\left(\frac{1}{2}mr^2 + me^2\right) \times \left(\frac{2\pi}{p}\right)^2\right](\ddot{z}_b - \ddot{z}_s) + c(\dot{z}_b - \dot{z}_u) = 0. \quad (5)$$

Then, the motion equations of the whole system are

$$\begin{cases} m_s\ddot{z}_s + k(z_s - z_u) + \left[\left(\frac{1}{2}mr^2 + me^2\right) \times \left(\frac{2\pi}{p}\right)^2\right](\ddot{z}_s - \ddot{z}_b) = 0, \\ \\ m_u\ddot{z}_u + k(z_u - z_s) + c(\dot{z}_u - \dot{z}_b) + k_t(z_u - z_r) = 0, \\ \\ \left[\left(\frac{1}{2}mr^2 + me^2\right) \times \left(\frac{2\pi}{p}\right)^2\right](\ddot{z}_b - \ddot{z}_s) + c(\dot{z}_b - \dot{z}_u) = 0. \end{cases}$$

$$(6)$$

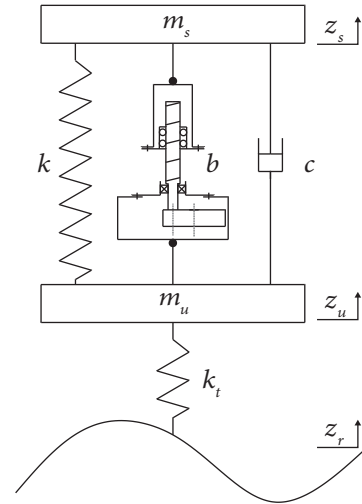Figure 3 shows a quarter car model with an eccentric inerter. In this model, the eccentric inerter is connected in parallel with the damping element. With the above analysis of the series-connected system, it is not difficult to find out the motion equation of this system.

For the sprung mass m_s, according to Newton's laws of kinematics, the equation is

$$m_s\ddot{z}_s + k(z_s - z_u) + c(\dot{z}_s - \dot{z}_u)$$

$$+ \left[\left(\frac{1}{2}mr^2 + me^2\right) \times \left(\frac{2\pi}{p}\right)^2\right](\ddot{z}_s - \ddot{z}_u) = 0. \quad (7)$$

For the unsprung mass m_u, the equation is

$$m_u\ddot{z}_u + k(z_u - z_s) + c(\dot{z}_u - \dot{z}_s) + k_t(z_u - z_r)$$

$$+\left[\left(\frac{1}{2}mr^2 + me^2\right) \times \left(\frac{2\pi}{p}\right)^2\right](\ddot{z}_u - \ddot{z}_s) = 0. \tag{8}$$

Then, the motion equations of the whole system are

$$\begin{cases} m_s\ddot{z}_s + k(z_s - z_u) + c(\dot{z}_s - \dot{z}_u) \\[2mm] \quad +\left[\left(\frac{1}{2}mr^2 + me^2\right) \times \left(\frac{2\pi}{p}\right)^2\right](\ddot{z}_s - \ddot{z}_u) = 0, \\[4mm] m_u\ddot{z}_u + k(z_u - z_s) + c(\dot{z}_u - \dot{z}_s) + k_t(z_u - z_r) \\[2mm] \quad +\left[\left(\frac{1}{2}mr^2 + me^2\right) \times \left(\frac{2\pi}{p}\right)^2\right](\ddot{z}_u - \ddot{z}_s) = 0. \end{cases} \tag{9}$$

3. Optimization of the Suspension Parameters

In order to explore the benefits of the vehicle ISD suspension employing the eccentric inerter, three performance indexes of the root mean square (RMS) values of the vehicle body acceleration, suspension working space, and dynamic tire load under the random road input are taken into consideration in the optimization process. Assuming the vehicle is driving at a speed of v on a Grade C road, the random road input is expressed as

$$\dot{z}_r(t) = -0.111\left[vz_r(t) + 40\sqrt{G_q(n_0)v}\,w(t)\right], \tag{10}$$

where $z_r(t)$ is the vertical displacement of the random road input, $G_q(n_0)$ is the road roughness, and $w(t)$ is the Gaussian white noise with mean value as 0. Here, $G_q(n_0)$ is $256 \times 10^{-6}\,\text{m}^3\cdot\text{cycle}^{-1}$, and v is 20 m/s. A genetic algorithm (GA) is a computational model of the biological evolutionary process that simulates the mechanism of natural selection and the genetics of Darwinian biological evolution and is a method to search for the optimal solution by simulating the natural evolutionary process. In this paper, the genetic algorithm is adopted to optimize the vehicle ISD suspension systems [30, 31].

3.1. Parameter Optimization of the Suspension with Series-Connected Eccentric Inerters. When using the genetic algorithm to determine the optimal parameters of the ISD suspension model with the series-connected eccentric inerter, the flywheel eccentricity e, the damping coefficient c, and the screw pitch p are set as the variables to be optimized, the remaining parameters of the suspension model are given in Table 1 [30], and the parameters of the ball-screw inerter are given by its common structure. Taking the traditional passive suspension as the comparison object, the RMS of the vehicle body acceleration, the suspension working space, and the dynamic tire load are used as optimization objectives, then establish a unified objective function, using MATLAB/Simulink to find the optimal solution of the objective function and its corresponding individual parameters.

TABLE 1: Parameters of the mature suspension model.

Parameter name	Value
Sprung mass m_s/kg	320
Unsprung mass m_u/kg	45
Stiffness of conventional spring k/(N·m^{-1})	22000
Stiffness of tire k_t/(N·m^{-1})	190000
Speed v/(m·s^{-1})	20
Roughness coefficient G_0/(m^3·cycle^{-1})	256×10^{-6}
Mass of the eccentric flywheel m/kg	0.4
Radius of the eccentric flywheel r/m	0.1

For the record, the RMS of the vehicle body acceleration, the suspension working space, and the dynamic tire load of conventional passive suspension under random road input is $1.3096\,\text{m·s}^{-2}$, 0.0130 m, and 900.47 N, respectively. Because the above three performance indexes have different units and orders of magnitude, it is necessary to establish a unified objective function. With the intention of exploring overall dynamic performances including ride comfort, handling stability, and driving safety of the proposed vehicle ISD suspension with eccentric inerters, the comprehensive objective is established. Divide the three indexes of the suspension with a series-connected eccentric inerter and the three indexes of the traditional passive suspension separately, and then take the sum of three quotients as the unified objective function. The unified objective function is used as the fitness function of the genetic algorithm. The expression of the unified objective function and its constraint conditions are as follows:

$$\begin{aligned} \min \quad & J = \frac{\text{BA}(X)}{\text{BA}_{\text{BD}}} + \frac{\text{SWS}(X)}{\text{SWS}_{\text{BD}}} + \frac{\text{DTL}(X)}{\text{DTL}_{\text{BD}}} + \text{punishment}, \\ & X = \begin{bmatrix} e & c & p \end{bmatrix}, \\ & lb < X_i < ub \quad i = 1, 2, 3, \end{aligned} \tag{11}$$

where J is the fitness function, BA(X), SWS(X), and DTL(X), respectively, represent the RMS of the body acceleration, the suspension working space, and the dynamic tire load of the vehicle ISD suspension with an eccentric inerter, and BA$_{\text{BD}}$, SWS$_{\text{BD}}$, and DTL$_{\text{BD}}$ are the RMS values of the vehicle body acceleration, the suspension working space, and the dynamic tire load of the conventional passive suspension, respectively. The punishment rule is decided that among the RMS of the body acceleration, the suspension working space, and the dynamic tire load, as long as one of them is inferior to the corresponding number of conventional passive suspension, the value of the punishment number is set as 100, or it is set as 0. X represents a set of parameters that need to be optimized, lb and ub represent the upper and lower limits of parameters to be optimized, respectively, considering the actual structure, thus lb = [0, 0, 0.005] and ub = [0.1, 4000, 0.03]. After determining the variables to be optimized, the fitness function, and the constraint conditions, the optimization results can be solved in MATLAB. The Pareto fraction is set as 0.3, the population size is set as 40, the stall gen limit is set at 200, and other parameters remain

unchanged. The optimal parameters of suspensions with series-connected eccentric inerters are listed in Table 2.

3.2. Parameter Optimization of the Suspension with a Parallel-Connected Eccentric Inerter.

The optimization method of the suspension with a parallel-connected eccentric inerter is the same as described above in 3.1, the variables to be optimized, the fitness function, and the constraint conditions are the same as well, and the optimization results can be solved. The optimal parameters of suspensions with parallel-connected eccentric inerters are listed in Table 3.

4. Dynamic Performance Analysis

To further study the performance improvement of suspensions with eccentric inerters and which connection structure is better for performance improvement, the vehicle ISD suspensions with a series-connected eccentric inerter and parallel-connected eccentric inerter are simulated both in the time and frequency domains using the optimized parameters from Section 3, respectively.

4.1. Simulation in Time Domain.

Figures 4–6 give the time-domain responses of vehicle body acceleration, suspension working space, and dynamic tire load of the ISD suspension compared to the passive suspension, where (a) is a series model and (b) is a parallel model.

Table 4 shows the dynamic performance indices of the optimized ISD suspension with a series-connected eccentric inerter and the optimized ISD suspension with a parallel-connected eccentric inerter.

It can be seen from the above figures and tables that for the optimized ISD suspension with a series-connected eccentric inerter, the dynamic performance indices are all decreased compared with the conventional suspension, the RMS of the body acceleration, the suspension working space, and the dynamic tire load is decreased by 2.0%, 10.0%, and 8.6%, respectively. For the optimized ISD suspension with a parallel-connected eccentric inerter, although the RMS of suspension working space was lowered by 28.4%, the body acceleration and the dynamic tire load have risen significantly, which is unfavorable for vehicle ride comfort and handling stability. A comparison of the two results reveals that the optimized ISD suspension with a series-connected eccentric inerter may have better overall dynamic performance; however, the ISD suspension with a parallel-connected eccentric inerter may deteriorate the working performance of the suspension.

4.2. Simulation in Frequency Domain.

Figures 7–9 show the gain of vehicle body acceleration, suspension working space, and dynamic tire load in the frequency domain, where (a) is a series model and (b) is a parallel model. In this part, in order to analyze the influence of eccentricity on the suspension performance, suspensions with eccentric inerters of two different eccentricities are analyzed as well besides the analysis of the conventional suspension and the suspension with optimized eccentric inerters.

TABLE 2: Optimal parameters of suspensions with series-connected eccentric inerters.

Optimized parameters	Value
Flywheel eccentricity e/m	0.046
Damping coefficient c/(N·s·m^{-1})	1317
Screw pitch p/m	0.015
Inertance b/kg	492

TABLE 3: Optimal parameters of suspensions with a parallel-connected eccentric inerter.

Optimized parameters	Value
Flywheel eccentricity e/m	0.0064
Damping coefficient c/(N·s·m^{-1})	1959
Screw pitch p/m	0.026
Inertance b/kg	117

For the responses in the frequency domain, with the increase of frequency, the gain value of the three indexes has the same change rule, that is, in the low-frequency band, it increases first and then decreases, and in the high-frequency band, it also shows a trend from rise to decline, and each frequency band has a peak value. From Table 5, for the vehicle body acceleration, the peak of the ISD suspension with a series-connected eccentric inerter in the low frequency is obviously lower than that of the conventional suspension, which decreases from 200.709 to 143.170 (m/s^2/m) (reduces by 28.7%), but for the high-frequency peak, the reformation is relatively small, from 611.320 to 596.701 (m/s^2/m) (reduces by 2.4%), and for different eccentricities, it can be found that two peaks increase gradually with the rise of eccentricity. The reformation of the suspension working space is more apparent compared to the vehicle's body acceleration. The low-frequency peak decreases from 2.725 to 2.176 (reduced by 20.1%), and the high-frequency peak decreases from 2.765 to 2.166 (reduces by 21.7%), and for different eccentricities, it can be found that two peaks show a trend of drop with the rise of eccentricity. For the dynamic tire load analysis, the low-frequency peak decreases from 66565.7 (N/m) to 48330.8 (N/m) (reduces by 27.4%), and the high-frequency peak decreases from 554541 (N/m) to 450385 (N/m) (reduces by 18.8%), and for different eccentricities, it can be found that the low-frequency peak increases with the rise of eccentricity, while the high-frequency peak shows a trend of drop. In general, the vibration isolation performance of the vehicle ISD suspension with a series-connected eccentric inerter is obviously improved in the frequency domain compared with the conventional suspension system. The suspension working space and the dynamic tire load are improved more apparently compared to the vehicle body acceleration. But for the vehicle ISD suspension with a parallel-connected eccentric inerter, the peak values of the gain of vehicle body acceleration, suspension working space, and dynamic tire load all soar in the range of 0–15 Hz and descend only in part of the high-frequency range, and with the rise of flywheel eccentricity, the peak value increases significantly. In a word, the ISD suspension with a parallel-connected eccentric inerter does not improve the overall dynamic performance of
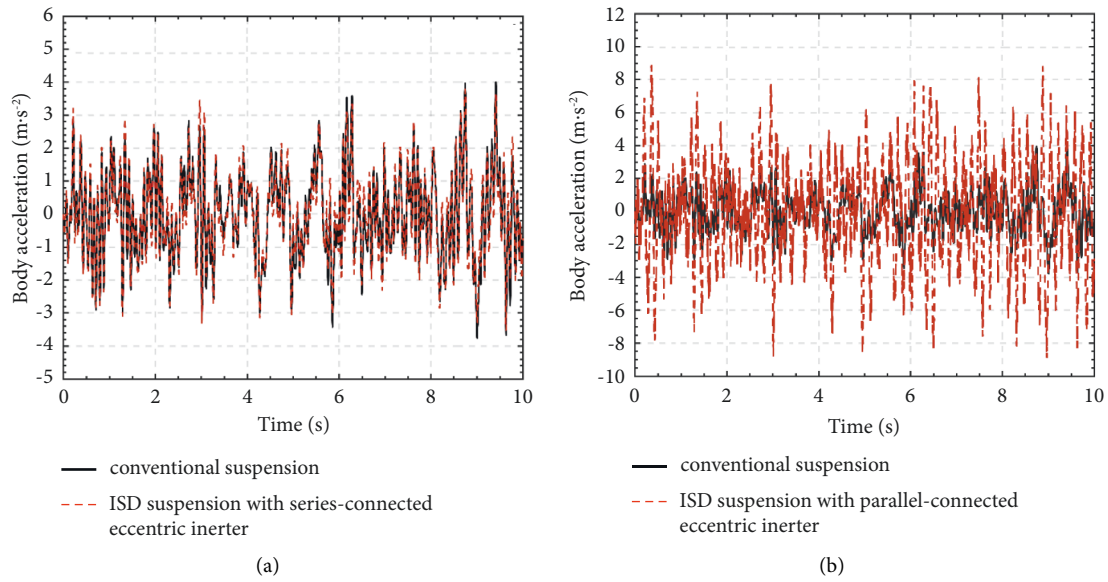
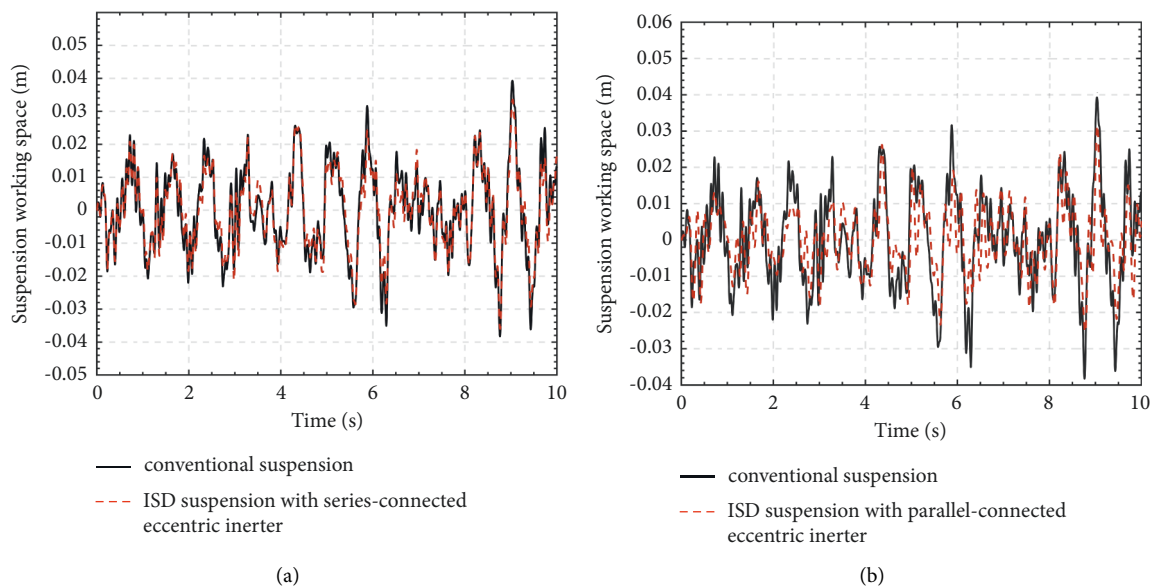FIGURE 4: Responses of vehicle body acceleration in time domain.

FIGURE 5: Responses of suspension working space in time domain.

the suspension, priority should be given to a series-connected eccentric inerter when improving suspension performance, which enables the suspension to achieve better overall dynamic performances, ride comfort, and handling stability.

5. Impact Analysis of the Parameters

The dynamic equations of the vehicle ISD suspension with series-connected and parallel-connected eccentric inerters show that the flywheel eccentricity and the screw pitch of the inerter determine the value of inertance, and the inertance directly affects the dynamic performance. Thus, to further study the impact of the flywheel eccentricity and the screw pitch on the body acceleration, the suspension working

space and the dynamic tire load, the value of inertance, and those three dynamic performance indices are deemed as response variables, while the eccentricity and screw pitch are deemed as independent variables. This paper makes the flywheel eccentricity change in the region of $[0, 0.1]$ m and the screw pitch change in $[0.005, 0.03]$m, the parameter selection is still consistent with Table 1, and the damping coefficient is consistent with Tables 2 and 3, respectively. Results and analysis are shown as follows.

5.1. Impact Analysis of Flywheel Eccentricity and Screw Pitch in Suspension with the Series-Connected Eccentric Inerter. Figure 10 shows the changing tendency of inertance b subject to the change of the flywheel eccentricity and the
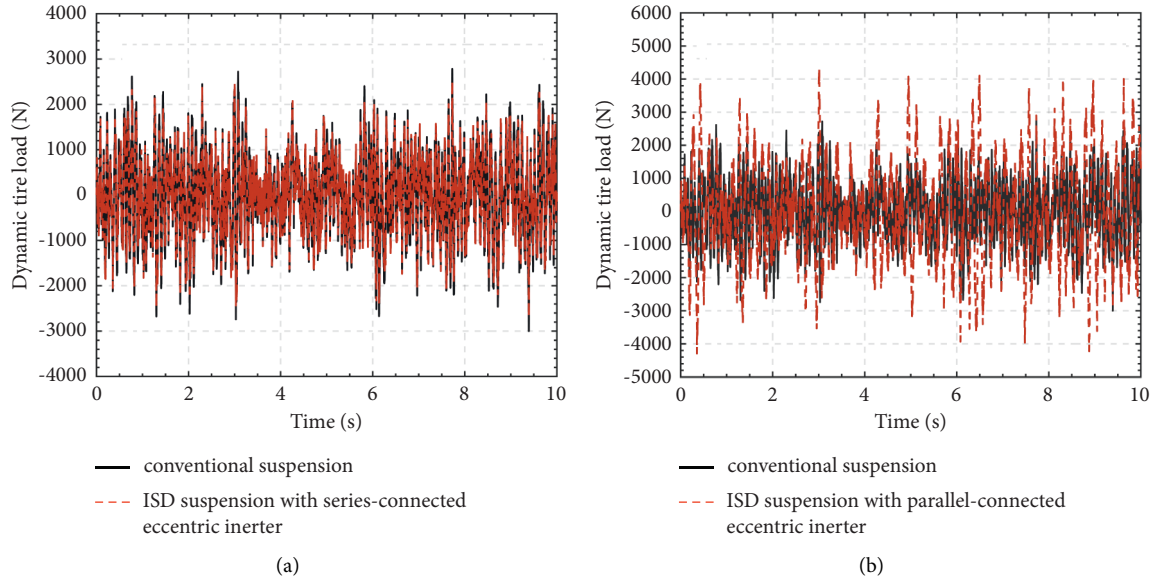
(a)

(b)

Figure 6: Responses of dynamic tire load in time domain.

Table 4: Dynamic performance indices.

Name	Conventional suspension	Series-connected inerter	Parallel-connected inerter
RMS of body acceleration/m·s^{-2}	1.3096	1.2834	3.0559
RMS of suspension working space/m	0.0130	0.0117	0.0093
RMS of dynamic tire load/N	900.47	822.61	1459.12

(a)

(b)
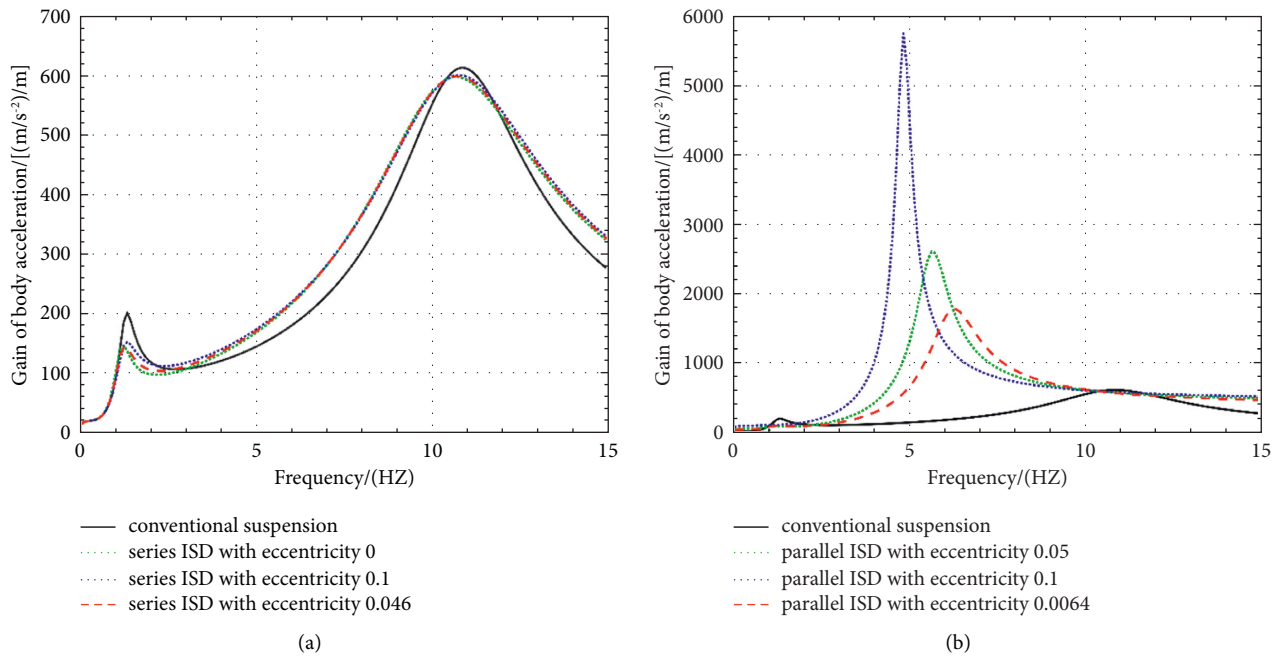
Figure 7: Responses of vehicle body acceleration in frequency domain.

screw pitch. It is shown that a large inertance value will be obtained with the increase of the flywheel eccentricity and the decrease of the screw pitch, which is consistent with (2).

Figures 11–13 show the changing tendency of three performance indices subject to the change of flywheel eccentricity and screw pitch; it is apparent from these figures that
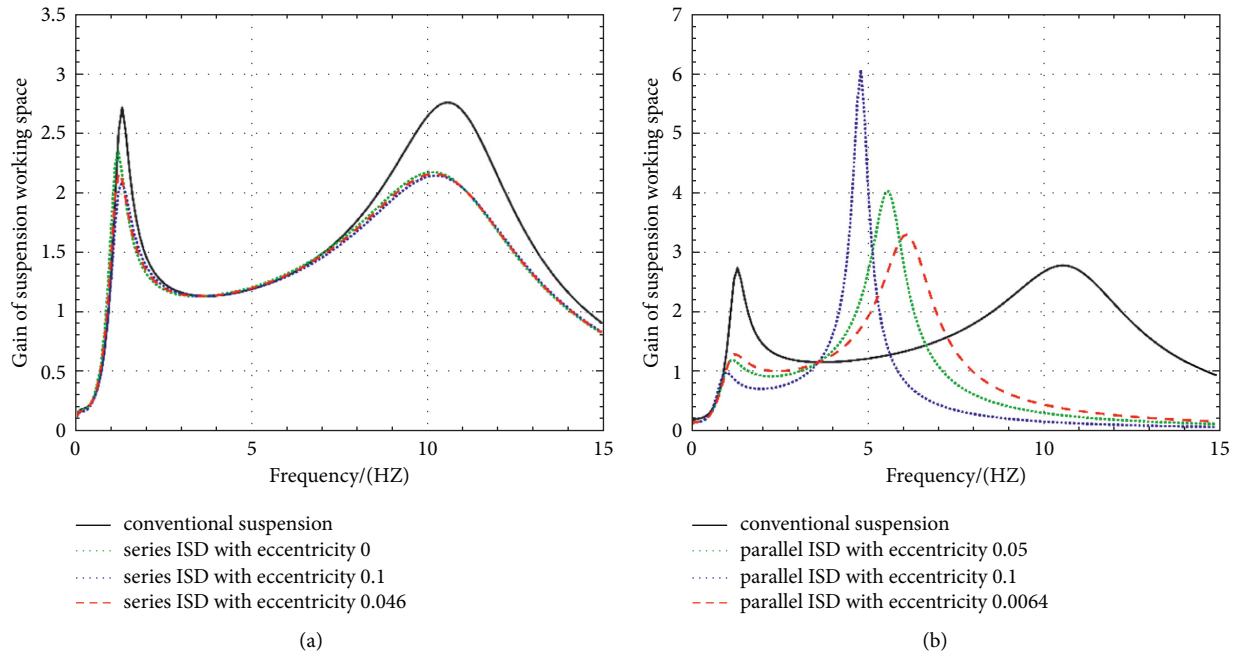
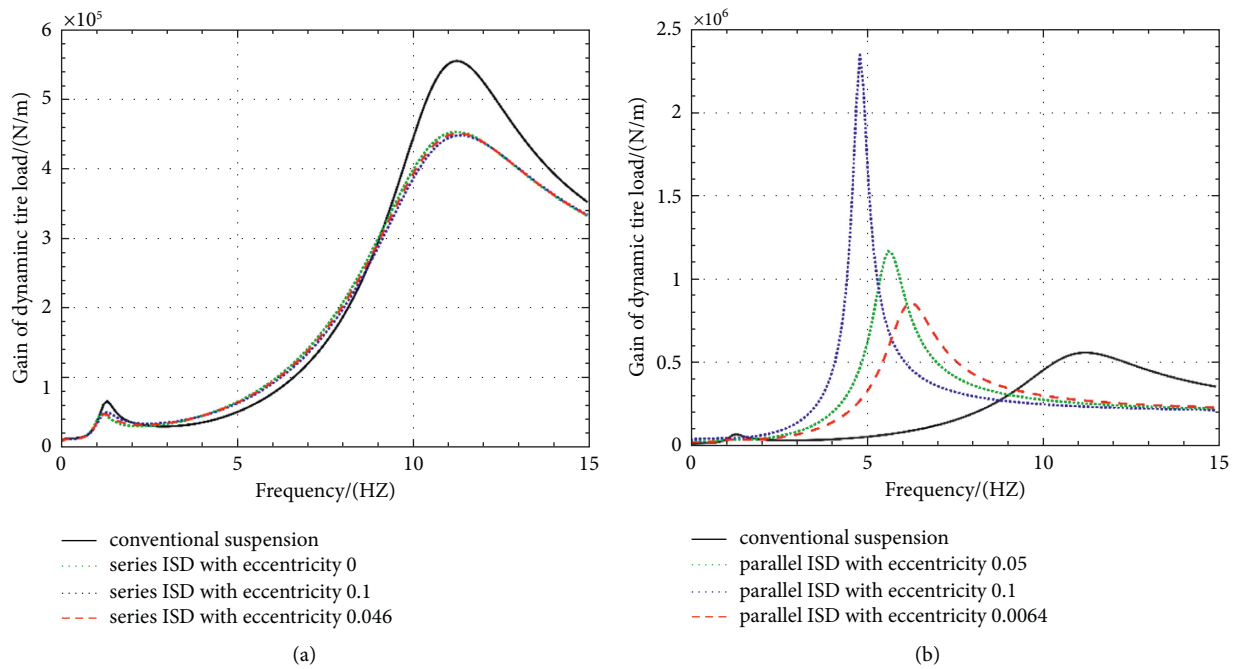FIGURE 8: Responses of suspension working space in frequency domain.

FIGURE 9: Responses of dynamic tire load in frequency domain.

TABLE 5: Comparisons of peak gain values in frequency domain in a series-connected suspension.

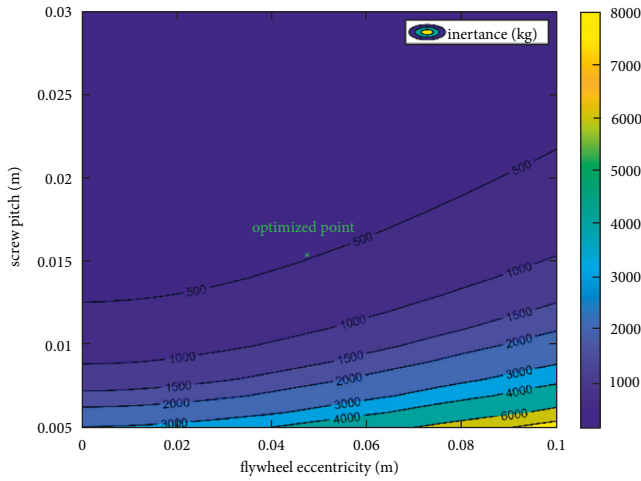| Name	Conventional suspension	ISD suspension with a series-connected inerter	Improvement (%)
Peak gain values of body acceleration/$(m/s^2/m)$	200.709	143.170	28.7
	611.320	596.701	2.4
Peak gain values of suspension working space	2.725	2.176	20.1
	2.765	2.166	21.7
Peak gain values of dynamic tire load (N/m)	66565.7	48330.8	27.4
	554541	450385	18.8

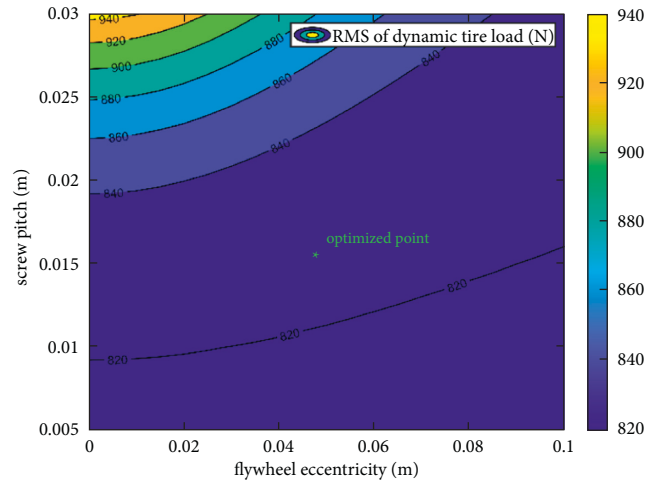FIGURE 10: The change of inertance subject to the change of flywheel and screw pitch.
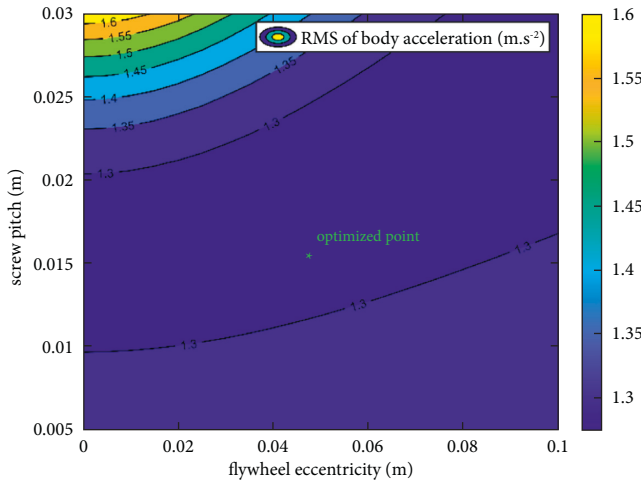

FIGURE 11: The change of body acceleration subject to the change of flywheel and screw pitch in the series model.

FIGURE 12: The change of suspension working space subject to the change of flywheel and screw pitch in the series model.

FIGURE 13: The change of dynamic tire load subject to the change of flywheel and screw pitch in the series model.
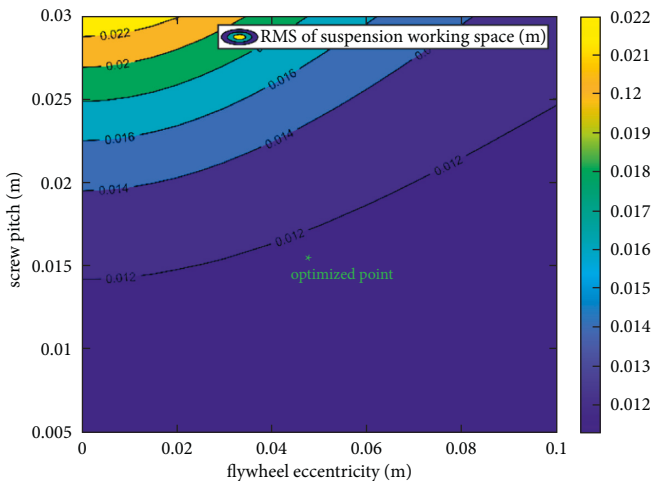
under the random road input, the RMS values of the vehicle body acceleration drop first and then ascend with the increase of the flywheel eccentricity and the screw pitch, and it reaches the lowest value when inertance b is within the region of [200,1000] kg. For the RMS of the suspension working space and the dynamic tire load, both of them have a trend of decline with the increase of flywheel eccentricity and have a trend of rising with the increase of screw pitch, which means that the bigger the inertance, the lower the values of these dynamic performance indices. Therefore, for the ISD suspension with a series-connected inerter, a reasonable selection of the flywheel eccentricity and screw pitch can keep the three dynamic performance indices at a small level, which is conducive to the improvement of the damping performance of the suspension, and attention should be paid to the design.

5.2. Impact Analysis of Flywheel Eccentricity and Screw Pitch in Suspension with the Parallel-Connected Eccentric Inerter. Figures 14–16 show the changing tendency of three performance indices subject to the change of the flywheel eccentricity and the screw pitch of the suspension with parallel-connected inerters. Overall, compared with the suspension with a series-connected inerter, the suspension with a parallel-connected inerter except for the RMS of suspension working space, which has decreased, the RMS values of body acceleration and dynamic tire load have soared substantially. For the RMS of suspension working space, although its value has a trend of decline with the increase of inertance, its range is less than 0.01 m, and the change is not obvious; however, the RMS of body acceleration and dynamic tire load significantly increased with rising inertance. Different trends are obtained in terms of the three performance indices, and the more detailed trade-off among the three performance indices needs to be discussed according to the different design guides.
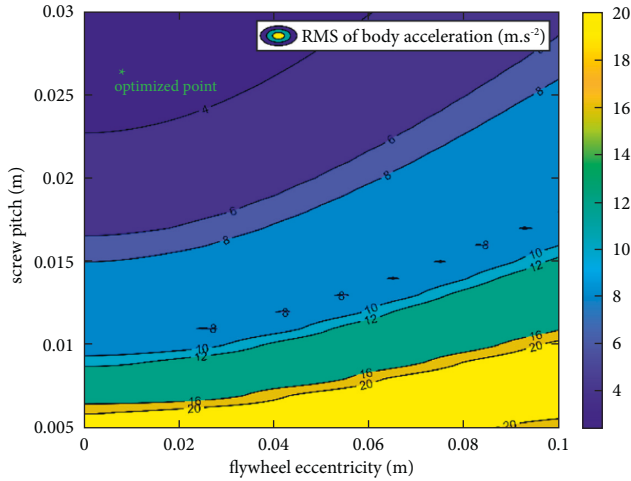
Figure 14: The change of body acceleration subject to the change of flywheel and screw pitch in the parallel model.
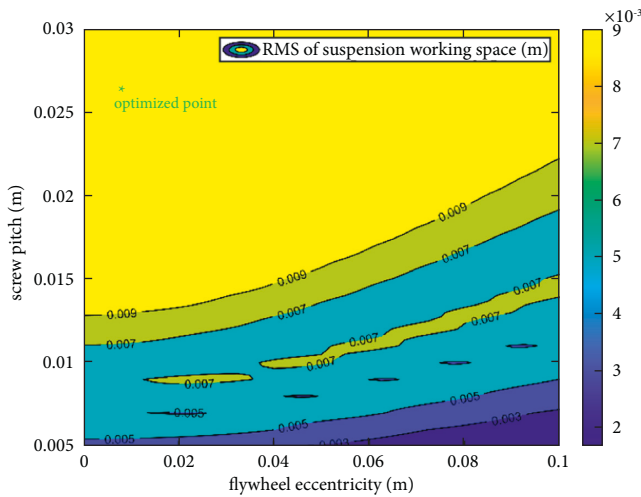

Figure 15: The change of suspension working space subject to the change of flywheel and screw pitch in the parallel model.
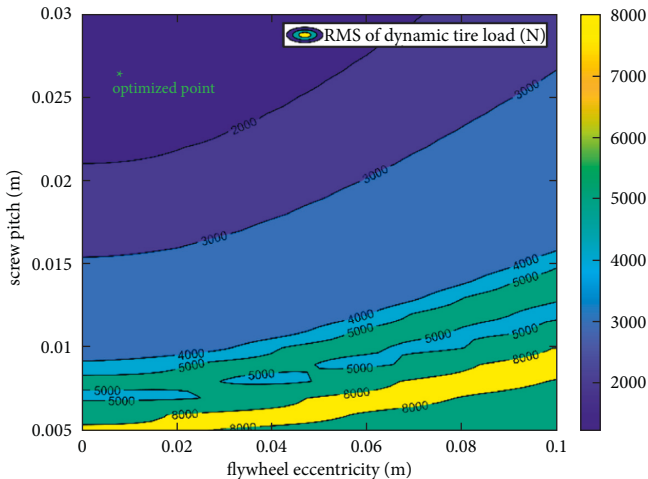

Figure 16: The change of dynamic tire load subject to the change of flywheel and screw pitch in the parallel model.

6. Conclusion

In this paper, the performance benefits of the vehicle suspension system employing an eccentric inerter are investigated. The quarter car models of the two basic vehicle ISD suspension layouts, namely the series-connected suspension and the parallel-connected suspension, are built. The key parameters of the two suspension systems are optimized by means of the genetic algorithm by considering the overall suspension performance. The simulation analysis of the two suspension models is carried out both in the time domain and the frequency domain, and the results show that the RMS of the body acceleration, the suspension working space, and the dynamic tire load of the series-connected layout vehicle ISD suspension decreased to varying degrees. The peak values of the body acceleration, the suspension working space, and the dynamic tire load in the lower frequency range are all significantly reduced, and the peak values in the high frequency range are all decreased as well. By comparing with the series-connected layout suspension, the improvement of the parallel-connected layout suspension is poor, which is not conducive to enhancing the comprehensive performance. At last, the influences of the change in the flywheel eccentricity and the screw pitch on the performance indices of the two suspension models are discussed in detail, which will provide a guide method for the suspension design.

Data Availability

The data used to support the findings of the study are available from the corresponding author upon request.

Conflicts of Interest

The authors declare that they have no conflicts of interest.

Acknowledgments

References

[1] M. Z. Q. Chen, Y. Hu, C. Li, and G. Chen, "Semi-active suspension with semi-active inerter and semi-active damper," *IFAC Proceedings Volumes*, vol. 47, no. 3, pp. 11225–11230, 2014.

[2] M. Ieluzzi, P. Turco, and M. Montiglio, "Development of a heavy truck semi-active suspension control," *Control Engineering Practice*, vol. 14, no. 3, pp. 305–312, 2006.

[3] X. J. Zhang, M. Ahmadian, and K. H. Guo, "On the benefits of semi-active suspensions with inerters," *Shock and Vibration*, vol. 19, no. 3, 272 pages, Article ID 640275, 2012.

[4] J. Cao, H. Liu, P. Li, and D. J. Brown, "State of the art in vehicle active suspension adaptive control systems based on intelligent methodologies," *IEEE Transactions on Intelligent Transportation Systems*, vol. 9, no. 3, pp. 392–405, 2008.

[5] Y. M. Sam, J. H. Osman, and M. A. Ghani, "A class of proportional-integral sliding mode control with application to

active suspension system," *Systems & Control Letters*, vol. 51, no. 3-4, pp. 217–223, 2004.

[6] W. Sun, Z. Zhao, and H. Gao, "Saturated adaptive robust control for active suspension systems," *IEEE Transactions on Industrial Electronics*, vol. 60, no. 9, pp. 3889–3896, 2013.

[7] M. C. Smith, "Synthesis of mechanical networks: the inerter," *IEEE Transactions on Automatic Control*, vol. 47, no. 10, pp. 1648–1662, 2002.

[8] M. Z. Q. Chen and Y. Hu, "Semi-active inerter and adaptive tuned vibration absorber," *Inerter and its Application in Vibration Control Systems*, pp. 103–119, Springer, Singapore, 2019.

[9] Y. Hu, T. Hua, M. Z. Q. Chen, S. Shi, and Y. Sun, "Instability analysis for semi-active control systems with semi-active inerters," *Nonlinear Dynamics*, vol. 105, no. 1, pp. 99–112, 2021.

[10] Y. Hu, T. Hua, M. Z. Q. Chen, S. Shi, and Y. Sun, "Inherent stability analysis for multibody systems with semi-active inerters," *Journal of Sound and Vibration*, vol. 535, Article ID 117073, 2022.

[11] X. L. Zhang, J. J. Liu, J. M. Nie, and L. Chen, "Design principle and method of a passive hybrid damping suspension system," *Applied Mechanics and Materials*, vol. 635-637, pp. 1232–1240, 2014.

[12] S. Djerouni, M. Abdeddaim, S. Elias, D. De Domenico, and R. Rupakhety, "Optimal seismic response control of adjacent buildings coupled with a double mass tuned damper inerter," *Optimization of Tuned Mass Dampers*, pp. 97–117, Springer, Cham, 2022.

[13] S. Djerouni, M. Abdeddaim, S. Elias, and R. Rupakhety, "Optimum double mass tuned damper inerter for control of structure subjected to ground motions," *Journal of Building Engineering*, vol. 44, Article ID 103259, 2021.

[14] S. Djerouni, S. Elias, M. Abdeddaim, and R. Rupakhety, "Optimal design and performance assessment of multiple tuned mass damper inerters to mitigate seismic pounding of adjacent buildings," *Journal of Building Engineering*, vol. 48, Article ID 103994, 2022.

[15] S. Djerouni, A. Ounis, S. Elias, M. Abdeddaim, and R. Rupakhety, "Optimization and performance assessment of tuned mass damper inerter systems for control of buildings subjected to pulse-like ground motions," *Structures*, vol. 38, pp. 139–156, 2022.

[16] T. D. Lewis, J. Z. Jiang, S. A. Neild, C. Gong, and S. D. Iwnicki, "Using an inerter-based suspension to improve both passenger comfort and track wear in railway vehicles," *Vehicle System Dynamics*, vol. 58, no. 3, pp. 472–493, 2020.

[17] A. Z. Matamoros-Sanchez and R. M. Goodall, "Novel mechatronic solutions incorporating inerters for railway vehicle vertical secondary suspensions," *Vehicle System Dynamics*, vol. 53, no. 2, pp. 113–136, 2015.

[18] F. C. Wang, M. K. Liao, B. H. Liao, W. J. Su, and H. A. Chan, "The performance improvements of train suspension systems with mechanical networks employing inerters," *Vehicle System Dynamics*, vol. 47, no. 7, pp. 805–830, 2009.

[19] X. Q. Sun, L. Chen, S. H. Wang, X. L. Zhang, and X. F. Yang, "Performance investigation of vehicle suspension system with nonlinear ball-screw inerter," *International Journal of Automotive Technology*, vol. 17, no. 3, pp. 399–408, 2016.

[20] S. J. Swift, M. C. Smith, A. R. Glover, C. Papageorgiou, B. Gartner, and N. E. Houghton, "Design and modelling of a fluid inerter," *International Journal of Control*, vol. 86, no. 11, pp. 2035–2051, 2013.

[21] F. C. Wang, M. F. Hong, and T. C. Lin, "Designing and testing a hydraulic inerter," *Proceedings of the Institution of Mechanical Engineers - Part C: Journal of Mechanical Engineering Science*, vol. 225, no. 1, pp. 66–72, 2011.

[22] R. Wang, X. Meng, D. Shi, X. Zhang, Y. Chen, and L. Chen, "Design and test of vehicle suspension system with inerters," *Proceedings of the Institution of Mechanical Engineers - Part C: Journal of Mechanical Engineering Science*, vol. 228, no. 15, pp. 2684–2689, 2014.

[23] L. Chen, C. Liu, W. Liu, J. Nie, Y. Shen, and G. Chen, "Network synthesis and parameter optimization for vehicle suspension with inerter," *Advances in Mechanical Engineering*, vol. 9, Article ID 168781401668470, 7 pages, 2017.

[24] R. Wang, Q. Ye, Z. Sun, W. Zhou, Y. Cao, and L. Chen, "A study of the hydraulically interconnected inerter-spring-damper suspension system," *Mechanics Based Design of Structures and Machines*, vol. 45, no. 4, pp. 415–429, 2017.

[25] X. Yang, L. Yan, Y. Shen, Y. Liu, and C. Liu, "Optimal design and dynamic control of an ISD vehicle suspension based on an ADD positive real network," *IEEE Access*, vol. 8, pp. 94294–94306, 2020.

[26] Y. J. Shen, J. Hua, Q. H. Hou, X. H. Xia, Y. L. Liu, and X. F. Yang, "Performance analysis of the fractional-order vehicle mechatronic ISD suspension with parameter perturbation," *Journal of Theoretical and Applied Mechanics*, vol. 60, pp. 141–152, 2022.

[27] Y. J. Shen, J. Hua, B. Wu, Z. Chen, X. X. Xiong, and L. Chen, "Optimal design of the vehicle mechatronic ISD suspension system using the structure-immittance approach," *Proceedings of the Institution of Mechanical Engineers - Part D: Journal of Automobile Engineering*, vol. 236, no. 4, pp. 512–521, 2022.

[28] Y. J. Shen, J. Z. Jiang, S. A. Neild, and L. Chen, "Vehicle vibration suppression using an inerter-based mechatronic device," *Proceedings of the Institution of Mechanical Engineers - Part D: Journal of Automobile Engineering*, vol. 234, no. 10-11, pp. 2592–2601, 2020.

[29] Y. J. Shen, Y. L. Liu, L. Chen, and X. F. Yang, "Optimal design and experimental research of vehicle suspension based on a hydraulic electric inerter," *Mechatronics*, vol. 61, pp. 12–19, 2019.

[30] Y. J. Shen, L. Chen, X. F. Yang, D. H. Shi, and J. Yang, "Improved design of dynamic vibration absorber by using the inerter and its application in vehicle suspension," *Journal of Sound and Vibration*, vol. 361, pp. 148–158, 2016.

[31] Y. J. Shen, M. Q. Jia, K. Yang, Z. Chen, and L. Chen, "Optimal design and dynamic performance analysis based on the asymmetric-damping vehicle ISD suspension," *Shock and Vibration*, vol. 202111 pages, Article ID 9996563, 2021.